SPE-233243-MS

A Novel Method for the Quantification of CO_2 Solubility in Hydrocarbon Phases Using the Drop Shape Analysis Technique

Ronghao Zhu and Hanin Samara, Institute of Subsurface Energy Systems, Clausthal University of Technology, Clausthal-Zellerfeld, Germany

 DOI 10.2118/233243-MS

This paper was prepared for presentation at the SPE Europe Energy Conference and Exhibition held in Istanbul, Turkiye, 23 - 25 June 2026.

Abstract

Carbon dioxide (CO_2) dissolution in hydrocarbons governs oil swelling and phase behavior in CO_2 enhanced oil recovery but quantifying CO_2-induced swelling and solubility remains challenging under high-pressure conditions. In this work, a captive bubble approach is employed to directly monitor hydrocarbon droplet expansion during CO_2 dissolution under controlled pressure and temperature conditions, spanning subcritical to supercritical CO_2 regimes and extending towards near-miscible conditions of the hydrocarbon-CO_2 mixture. Experiments are conducted for n-decane ($C_{10}H_{22}$) and n-hexadecane ($C_{16}H_{34}$). Based on droplet expansion measurements combined with density data, a practical workflow is proposed to determine CO_2 solubility in the oleic phase. The results show that pressure enhances CO_2 dissolution and accordingly oil droplet swelling, whereas increasing temperature weakens dissolution and expansion. A clear chain-length dependence is observed, with n-decane exhibiting higher CO_2 solubility and greater swelling than n-hexadecane. Notably, under selected near-miscible conditions, continuous droplet expansion without a distinct plateau is observed, suggesting deviations from a simple equilibrium dissolution picture. Overall, this study provides a novel experimental methodology for quantifying CO_2 solubility and swelling while highlighting complex swelling behavior near conditions of complete miscibility.

Introduction

Carbon dioxide Enhanced Oil Recovery (CO_2-EOR) has long been regarded as an effective method for increasing oil recovery. In addition to viscosity reduction and interfacial tension related mechanisms, the dissolution of CO_2 can cause volumetric expansion of dispersed oil, which may subsequently coalesce into a continuous phase with improved mobility (Fig 1). Therefore, accurate knowledge of CO_2 solubility and the associated swelling behavior of hydrocarbons is essential for understanding and optimizing CO_2-EOR processes. Furthermore, CO_2 dissolution into reservoir fluids also represents a potential mechanism for carbon storage during EOR operations, since part of the injected CO_2 can be retained in the oleic phase. Reliable solubility data are important not only for enhanced oil recovery performance, but also for evaluating CO_2 storage efficiency in coupled CO_2-EOR and carbon capture and storage (CCS) scenarios.

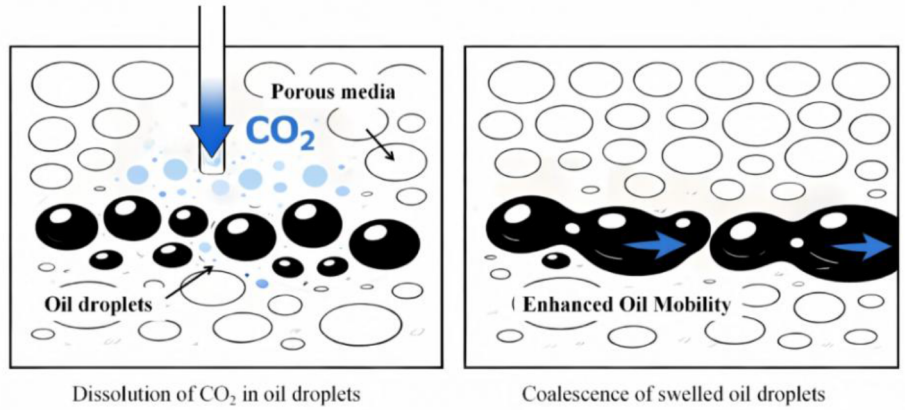

Figure 1—Schematic illustration of CO_2 dissolution, oil droplet swelling, and coalescence in porous media.

Despite extensive research, quantifying CO_2 dissolution and swelling remains challenging, particularly under high-pressure conditions, where experimental datasets obtained with different methodologies are not always consistent. Moreover, several conventional solubility measurement methods require sampling, indirect compositional analysis, or model-dependent interpretation, which may introduce uncertainties and limit comparability across studies. In this study, the captive bubble method is employed to directly quantify the volumetric expansion upon CO_2 dissolution at sub and supercritical CO_2 conditions. The experiments are conducted up to the so-called minimum miscibility pressure (MMP). Oil phases under investigation are n-decane ($C_{10}H_{22}$) and n-hexadecane ($C_{16}H_{34}$). Moreover, an experimental workflow is developed to determine the solubility of CO_2 in the oil phase by combining the measured volumetric expansion to the densities of the respective systems.

Summary of previous studies

Depending on research objectives, previous studies employed different oil systems (e.g., crude oils, pure hydrocarbons or binary mixtures thereof) and experimental methodologies. Therefore, a structured review is necessary to summarize key findings and identify limitations relevant to the present work. Several studies have focused on CO_2 dissolution behavior in light hydrocarbons and crude oils. For instance, Fu et al. investigated CO_2 solubility in crude oil under high-pressure conditions, discussed the relationship between oil swelling and viscosity, and demonstrated the positive impact of this mechanism on EOR (Fu et al., 2024). Barclay compiled published datasets to develop an empirical correlation for predicting CO_2 solubility in light crude oils (Barclay & Mishra, 2016). In addition, Mahdaviara et al. employed machine learning models to predict CO_2 solubility in oil systems with improved accuracy compared to conventional correlations (Mahdaviara et al., 2021).

While these studies provide valuable insights, crude oils are compositionally complex and vary significantly across reservoirs, which complicates the accurate determination of CO_2 solubility and limits direct comparability between datasets (Hu et al., 2017). For this reason, model oils, especially pure n-alkanes, are often used to establish fundamental solubility trends and to support the validation of predictive models. In this study, n-decane ($C_{10}H_{22}$) and n-hexadecane ($C_{16}H_{34}$) were selected as representative medium and long chain alkanes (Simoncelli et al., 2020). These two n-alkanes are widely used as model components for crude oils because they represent the typical range of aliphatic hydrocarbons and allow the chain-length effect to be studied under well-controlled conditions. Table 1 summarizes representative experimental approaches and key findings reported for CO_2 dissolution or interaction in n-decane, n-hexadecane, and closely related n-alkanes. It also specifically summarizes the research methodologies, conditions, and conclusions of this series of studies. A review of these research methods reveals a consistent lack of experimental techniques capable of directly observing the dissolution of carbon dioxide and the expansion of

hydrocarbon samples caused by this dissolution. To address this research gap, this study primarily utilizes a visual observation through adopting the captive bubble method, which enables simultaneous determination of solubility and swelling under controlled pressure and temperature conditions. The basic method of calculation, experimental setup and procedures are presented in the following chapter.

Table 1—Previous studies on interaction of CO_2 into n-decane or n-hexadecane.

Reference	Property	Hydrocarbon Type	Method	Pressure	Temperature	Conclusion
(Wang et al., 2023)	CO_2 solubility in n-decane and mixture system of n-decane and n-hexane as a cosolvent	n-decane (C_{10}) and n-decane(C_{10})+ n-hexane(C_6)	In situ Raman spectroscopy	0-150 bar	30-80 °C	Cosolvent (n-hexane) could increase CO_2 solubility; provided precise solubility data
(Nourozieh et al., 2013)	CO_2 solubility & density	n-decane(C_{10}), n-octadecane(C_{18})	PVT Phase Equilibrium Method; Fitting with Equation of State (SRK) and (PR)	0-60 bar	100 °C	Solubility of CO_2 increases with increasing pressureand reduces with the molecular weight. PR & SRK EOS accurately estimate solubility and densities
(Chou et al., 1990)	High-pressure vapor-liquid equilibria (VLE) expeiments for CO_2/hydrocarbon binary and ternary systems	n-decane(C_{10}), tetralin($C_{10}H_{12}$)	Static equilibrium	40-244 bar	71.1 °C and 104.4 °C	CO_2 is more soluble in n-decane than in teralin
(Shi et al., 2015)	Solubility of a series of n-alkanes in Supercritical CO_2	n-hexane (C_6), n-octane (C_8), n-decane (C_{10}), n-dodecane (C_{12}), n-tetradecane (C_{14}), n-hexadecane (C_{16}), n-octadecane (C_{18})	Observation in view chamber. Chrastil model to estimate the relationship of CO_2 density and its solubility.	50 - 200 bar	45 - 70 °C	Solubility increases with P, decreases with T and chain length; The density of CO_2 is positively correlated with its solubility
(He et al., 2021)	CO_2 solubility in heavy n-alkanes	n-hexadecane(C_{16}), n-heptadecane(C_{17}), n-octadecane(C_{18}), n-nonadecane(C_{19}), n-eicosane(C_{20})	Constant volume apparatus	up to 237.3 bar	60 -100 °C	CO_2 solubility increases with pressure, decreases with increasing alkane chain length and temperature. The dissolution process is associated with a negative entropy change.
(Siqueira Campos et al., 2009)	CO_2 solubility in water and hexadecane	n-hexadecane(C_{16})	Gas–liquid equilibrium apparatus and pressure–decay solubility measurement	0.517–5.354 bar	30 - 50 °C	Accurate solubility data for carbon dioxide in both water and hexadecane at low pressures and temperatures
(Mejía et al., 2014)	Interfacial properties of CO_2 with decane and CO_2 with eicosane	n-decane (C_{10}) n-eicosane(C_{20})	High-pressure pendant drop tensiometer and densimeter	1-100 bar	70 °C (n-decane) 30 °C (n-eicosane)	Experiments provided reliable data, simulations uncover molecular-scale details. CO_2 has stronger surface adsorption in long-chain alkanes (eicosane).
(Mohammed et al., 2017)	Viscosities and densities of hexadecane with dissolved methane or carbon dioxide	n-hexadecane (C_{16})	Vibrating-wire viscometer/ densimeter	Up to 1200 bar	25 to 200 °C	Measurements of viscosity and density were successfully performed. Data were correlated using modified Tait and Tait–Andrade equations.
(Sebastian et al., 1980)	Vapor-liquid equilibrium for CO_2 + n-decane and CO_2 + n-hexadecane	n-decane (C_{10}), n-hexadecane (C_{16})	Flow-type apparatus with gas chromatography analysis	20.3–50.7 bar	189–391°C	VLE data were successfully measured. CO_2 solubility increases with P, decreases with increasing T. Results for CO_2 + n-decane agree well with earlier literature data.

Materials and methods

Materials

Fluid. The gas employed in this study was carbon dioxide (CO_2) with a purity of 99.99%, supplied by Westfalen AG, Germany. Distilled water was acquired from the chemical storage facility of TU Clausthal. n-Decane with a purity of 99% was supplied by Thermo Scientific, and n-Hexadecane with 99% purity was obtained from Alfa Aesar GmbH.

Solid. A high-purity calcite crystal was used as a physical constraint, preventing the formed droplet from rising due to buoyancy caused by the density difference between the hydrocarbon and water phases. Given the extremely low porosity and permeability of the calcite crystal sample and its water-wet characteristic, the hydrocarbon droplet is prevented from penetrating into the rock matrix. Accordingly, any volume loss during the measurements is avoided.

Methods

Volumetric expansion. Determination of the volume expansion was performed using the captive bubble method, which is a direct visual observation technique (Fig. 2). The experiments were performed using a drop shape analysis system (DSA100, Krüss, GmbH). equipped with a high-pressure and high-temperature view chamber supplemented with sapphire windows (PDE-1700 MD-H, Eurotechnica GmbH, Germany). The view chamber was surrounded by an optical system for drop shape analysis, enabling continuous observation and monitoring of the droplet. The optical system includes dual switchable light sources, and a charge-coupled device camera with 1920 × 1200 pixels, a zoom function unit, and a high-resolution adjustment module. The system provides a volume resolution of up to 10^{-3} µL, ensuring accurate determination of droplet volume under experimental conditions. At the top of the view chamber, a minidosing device is installed, through which a small amount of liquid sample (oil) can be injected into the chamber via a movable capillary. The movable capillary is located at the bottom of the view chamber and is connected to the minidosing unit, providing an additional flow channel for liquid hydrocarbon injection and adjustment during the experiment. To maintain and precisely control the gas pressure, the view cell was connected to a syringe pump (260D-ISCO, Teledyne, USA), which allows precise control of gas pressure, gas flow rate, and the injected gas volume. In addition, a piston hand pump is installed at the bottom of PDE and connected to the view chamber. This hand pump is used to initially fill the chamber with the liquid sample (water) and to adjust the liquid volume as required. Temperature control is achieved using a heating jacket paired with a PID temperature controller. A thermocouple installed inside the view chamber provides temperature measurements with a resolution of ± 0.1 °C. The pressure inside the chamber is monitored by a pressure sensor (WIKA, Germany) with an accuracy of 0.1% full scale (600 bar). The real-time pressure and temperature data are continuously displayed on the ADVANCE software interface (Krüss, GmbH).

Prior to each experiment, the view chamber and all connected pipelines were thoroughly cleaned to eliminate any potential contamination. The system temperature was then set to the target experimental value, and sufficient time was allowed for thermal stabilization. After opening the view cell, the calcite rock sample was placed inside the chamber. The rock surface was carefully adjusted to a horizontal position to ensure a stable placement of the hydrocarbon droplet at the center of the view cell. Once the sample was correctly positioned, the view cell was sealed by closing the sapphire windows. Subsequently, the fluid injection system was prepared before the experiment. This preparation included confirming the availability of CO_2 in the syringe gas pump, ensuring that distilled water was charged into the bottom hand pump, and filling the minidosing pump with the hydrocarbon sample. After completion of the preparation steps, distilled water was then slowly pumped into the view chamber using the hand pump. The view chamber was first filled

with water to approximately 80% of its volume, ensuring that the water level completely submerged the bottom surface of the rock sample yet leaving room for the formation of a gas cap.

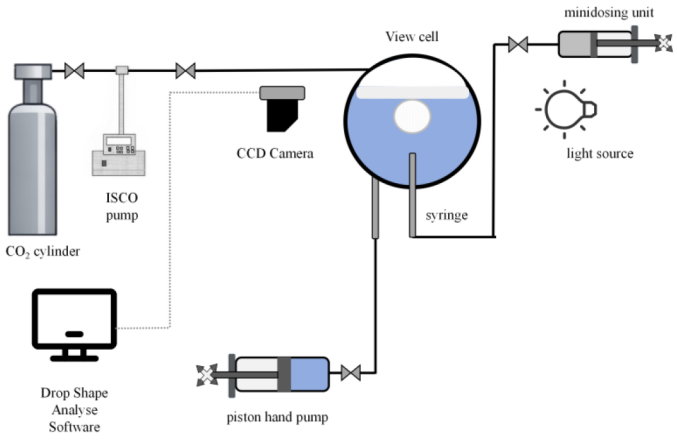

Figure 2—Schematic diagram of the complete experimental setup.

The hydrocarbon phase was subsequently introduced into the view cell through the minidosing pump unit. The volume of the hydrocarbon droplet was controlled by adjusting the pumping rate. Once the hydrocarbon droplet formed at the tip of the capillary, the capillary was slowly raised until the droplet gently contacted the rock surface. Pumping of the hydrocarbon was continued until the target droplet volume was reached. Afterwards, the capillary tube was then slowly retracted. Subsequently, CO_2 was introduced into the view chamber until the pressure reached the desired value. The software continuously detects the exact profile of the hydrocarbon sample droplet and records its volume. Using ADVANCE software, the theoretical baseline for drop shape analysis was adjusted to ensure parallel alignment with the rock surface. Subsequently, the focus of the optical system was gradually refined using the resolution control until the droplet, located at the center of the field of view, was sharply resolved. In Fig. 3 A droplet of n-hexadecane deposited on the calcite surface and immersed in distilled water inside the view chamber is exemplarily shown.

Figure 3—Representative image of a captive bubble of n-hexadecane in distilled water.

As CO_2 was introduced into the system, it dissolved into the surrounding distilled water and subsequently into the hydrocarbon droplet, resulting in a gradual increase in droplet volume. The pressure inside the view chamber was maintained at the design value using the syringe pump, which continuously supplied CO_2 to the system to compensate for pressure drop due to gas dissolution into the liquid phases, thereby ensuring an unlimited supply of the gas and constant pressure conditions. The droplet volume was recorded as a function of time to track the expansion process upon CO_2 dissolution. When the droplet volume became constant, it had reached thermodynamic equilibrium. The final stable volume was then used for subsequent analysis. Upon completion of each measurement, the system was depressurized and thoroughly cleaned in preparation

for the next experimental condition to be tested. For this series of volumetric expansion experiments, an initial pressure of 20 bar was selected, after which the system pressure was increased stepwise in increments of 20 bar until near-miscible conditions are reached. Experiments were conducted at two temperatures, namely 40 °C and 60 °C, in order to investigate the temperature dependence of CO_2 dissolution behavior. Each measurement was performed in duplicate to ensure reproducibility.

Density. An oscillating U-tube densitometer (DMA-HPM, Anton Paar, Austria) was used to measure the pure phase density of these two hydrocarbon samples ($C_{10}H_{22}$ and $C_{16}H_{34}$) under pressure (without CO_2) at 40 and 60 °C. The U-tube operates at pressures up to 140 MPa and temperatures up to 200 °C, providing a density resolution of 1 x 10^{-4} g/cm^3. Temperature and pressure within the densitometer system were monitored using a thermocouple with a resolution of 0.01°C and a pressure transducer with a resolution of 0.01 bar, respectively. The oscillating tube densitometer was connected to a minidosing unit, identical to that used in the captive bubble experiments, which was used to charge the oscillating tube with the hydrocarbon of interest and subsequently pressurize it. In each density measurement, the drainage valve (V2) was kept open prior to pressurization to flush the entire system with the hydrocarbon of interest and displace air previously present in the system. Afterwards, V2 was closed and the pressure was gradually increased by pumping more liquid into the system until the target pressure was reached. Subsequently, the inlet valve (V1) was closed to maintain the stable pressure inside the U-Tube. To ensure uniform temperature distribution, the entire experimental setup was placed in a hot-air bath oven system during the measurement process. A schematic diagram of the U-tube densitometer setup is shown in Fig. 4. Once the target pressure was reached and the density readings became stable, data were recorded. At each pressure level, four to five measurements were collected to ensure measurement reliability and repeatability, and the average value was used for further analysis. The measured pressure steps were identical to those used in the volumetric expansion experiments, with an initial pressure of 20 bar.

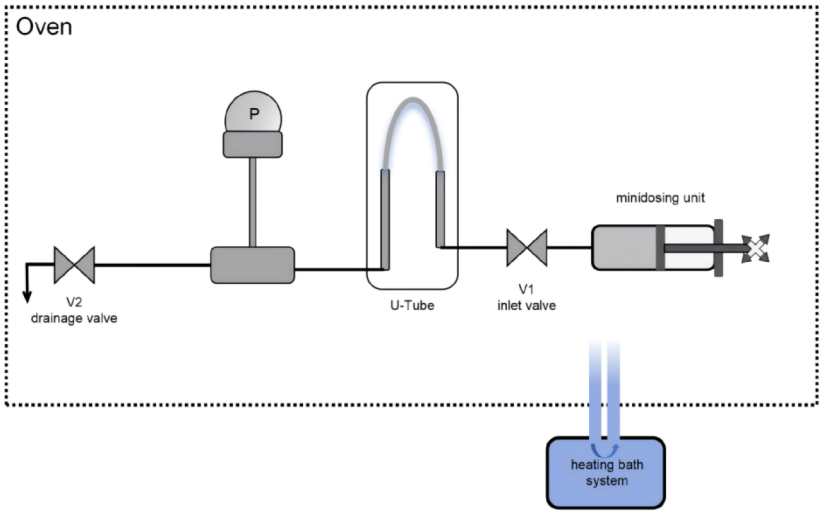

Figure 4—Schematic Diagram of U-Tube Density Measurement Device.

Carbon dioxide solubility. The CO_2 solubility was determined using the measured volumetric expansion of the hydrocarbon droplet and the corresponding density data. The initial mass of the pure hydrocarbon droplet is given by:

$$m_o = \rho_o V_o , \quad \text{(Eq. 1)}$$

where m_o is mass of the droplet, ρ_o is the density of the pure hydrocarbon and V_o is the initial droplet volume under initial condition (directly after pressurization but prior to CO_2 dissolution). After CO_2 dissolution, the

droplet volume increases resulting in its volumetric expansion. The initial droplet volume is denoted as V_o, and the final droplet volume at equilibrium is expressed as V_{sat}. Correspondingly, the volumetric expansion ratio is denoted as V_{exp}, and the equation is given as follows:

$$V_{exp} = \frac{V_{sat}}{V_o}, \quad \text{(Eq. 2)}$$

The density of the CO_2 saturated hydrocarbon phase is denoted as ρ_{sat}. Accordingly, the total mass of the droplet m_{sat} is expressed as:

$$m_{sat} = m_o + m_{CO_2} = \rho_{sat} V_{sat}, \quad \text{(Eq. 3)}$$

Substituting equation 2 into equation 3 yields:

$$m_o + m_{CO_2} = \rho_{sat} \quad V_o \cdot V_{exp}, \quad \text{(Eq. 4)}$$

Substituting V_o with ρ_o from equation 1 and rearranging equation 4 yields the CO_2 solubility (S) in the hydrocarbon phase in g/g.

$$S = \frac{m_{CO_2}}{m_o} = \left(\frac{\rho_{sat}}{\rho_o}\right)\left(V_{exp}\right) - 1 \quad \text{(Eq. 5)}$$

Results and data analysis

Density

This section presents the density values of pure n-decane and n-hexadecane as a function of pressure and temperature. The results are compared with reference values reported in the NIST database and published literature (Linstrom & Mallard, 1997) (Outcalt et al., 2010) as shown in Fig. 5 and Fig. 6. Within the investigated pressure range and at constant temperature, an approximately linear relationship between density and pressure was observed. The measured densities are in close agreement with the NIST reference data, with a maximum deviation of less than 0.5%. As shown in the methods section, to determine the solubility of carbon dioxide, it is also necessary to measure the density of the hydrocarbon phase after saturation with CO_2 under corresponding pressure and temperature conditions. In this work, only pure hydrocarbon densities as a function of pressure and temperature were determined. For the CO_2-saturated hydrocarbon densities, previously reported data by (Ahmadyar & Samara, 2025) were utilized, as several of the required density values were reported under pressure and temperature conditions comparable to those investigated in the present work. In the absence of experimentally determined density data for the CO_2-saturated hydrocarbon phase under comparable conditions, a linear regression model was applied to the available data set in (Ahmadyar & Samara, 2025). The missing density values were subsequently estimated using the derived linear regression relationship as shown in Fig. 7.

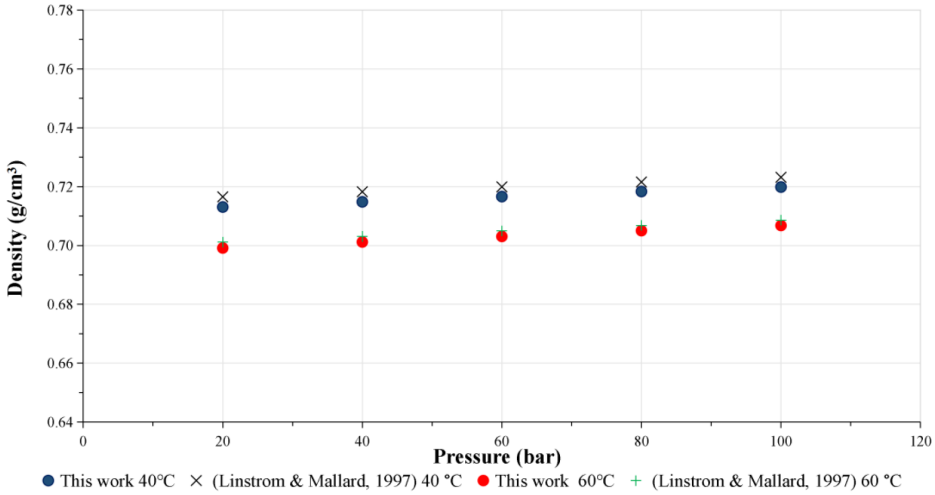

Figure 5—Pure phase density of n-decane at 40 °C and 60 °C as a function of pressure.

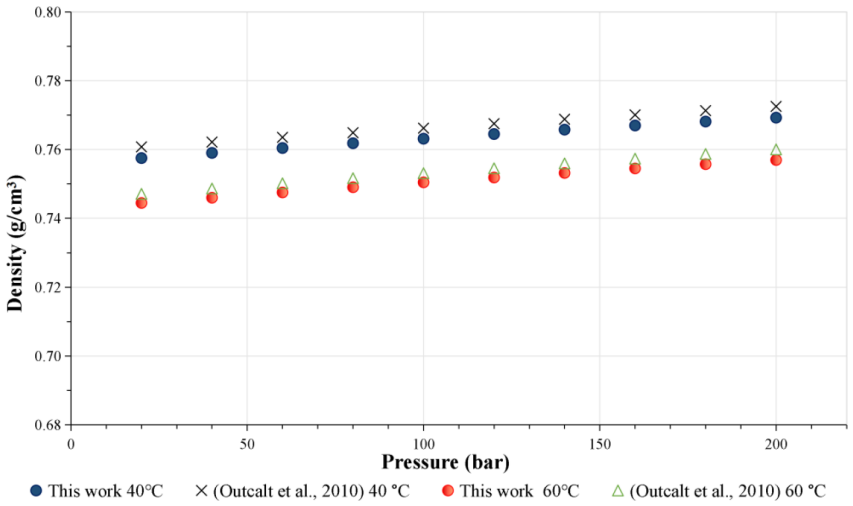

Figure 6—Pure phase density of n-hexadecane at 40 °C and 60 °C as a function of pressure.

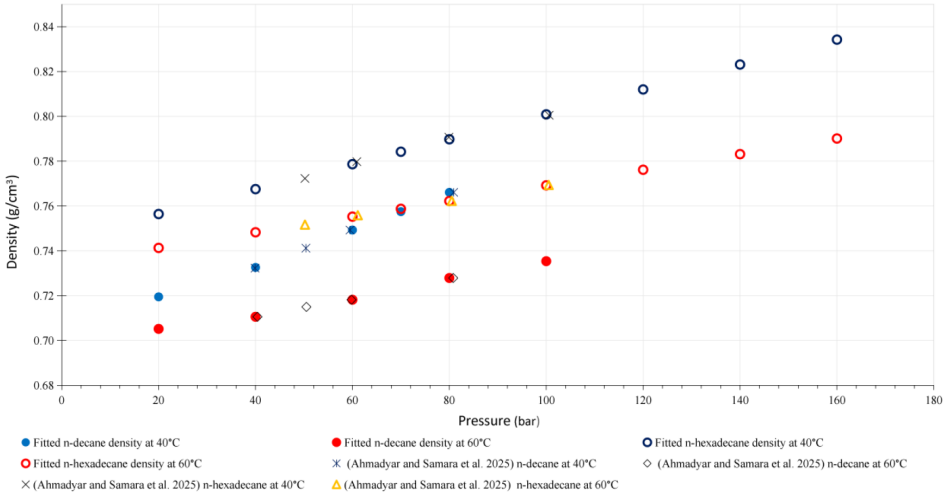

Figure 7—Density values adapted from (Ahmadyar & Samara, 2025) and linearly regressed density for CO_2 saturated n-decane and n-hexadecane at 40 °C and 60 °C.

Volumetric expansion

Based on Eq. 2, the volumetric expansion of the hydrocarbon was quantified by relating the final saturated volume of the droplet to its initial volume. The swelling behavior of the oil droplets under different pressures and temperatures is presented in Fig. 8. The volumetric expansion ratio increases with pressure for both hydrocarbons, indicating enhanced CO_2 dissolution at higher pressures. At 40 °C, n-decane exhibits significantly greater expansion than n-hexadecane, with the expansion ratio rising sharply at elevated pressures. Additionally, the measurement results indicate that the shorter chain alkane (n-decane) exhibits higher volumetric expansion compared to longer chain alkane (n-hexadecane), while the expansion decreases with increasing temperature.

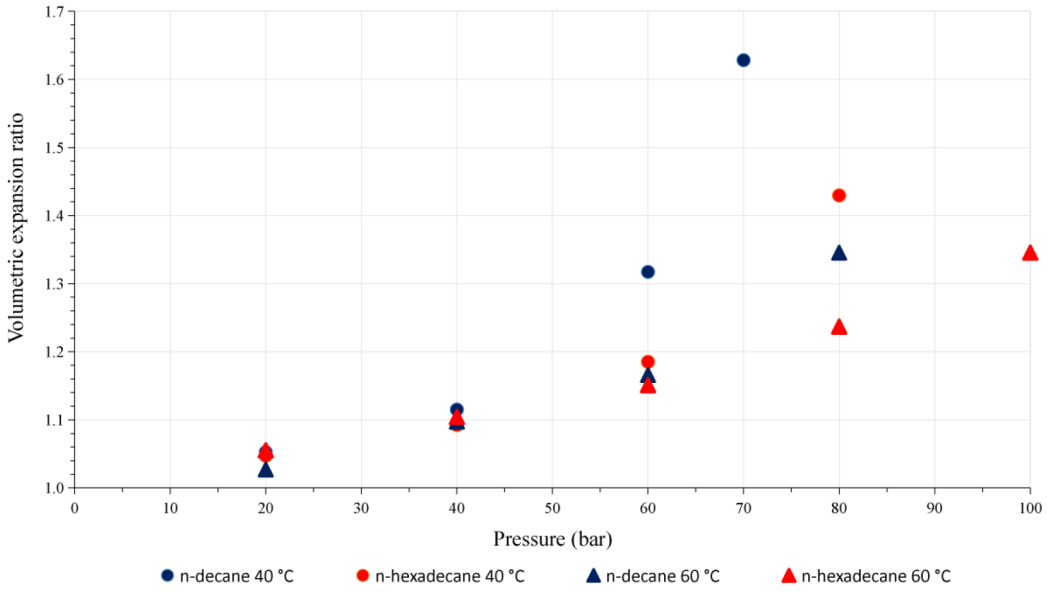

Figure 8—Volumetric expansion ratio of n-decane and n-hexadecane at 40 °C and 60 °C under different pressures.

Carbon dioxide solubility

Based on the approach described in the previous section, the measured volumetric expansion ratios V_{exp} were combined with the corresponding density data to quantify solubility of CO_2 in the hydrocarbon phase. The solubility values are for n-decane and n-hexadecane at 40 °C and 60 °C are shown in Fig. 9, and the calculated values are compared against the literature values reported in previous works (Wang et al., 2017; Jiménez-Gallegos et al., 2006; Pan & Trusler, 2023; Charoensombut-amon et al., 1986; Liu et al., 2024; Tanaka et al., 1993; Kobayashi & Firoozabadi, 2022) as shown in Fig.10–13. The values exhibit excellent agreement with those reported in (Wang et al., 2017) and (Charoensombut-amon et al., 1986). It should be noted that literature datasets are not fully consistent in terms of measurement conditions and methodology. Some reference data are not directly obtained from experiments. For instance, the data provided by Pan et al. (Pan & Trusler, 2023) were obtained from EOS phase equilibrium calculations rather than direct solubility measurements. Therefore, these data are utilized for qualitative trend comparison only. Nevertheless, the overall trend remains consistent, supporting the reliability of the present solubility results.

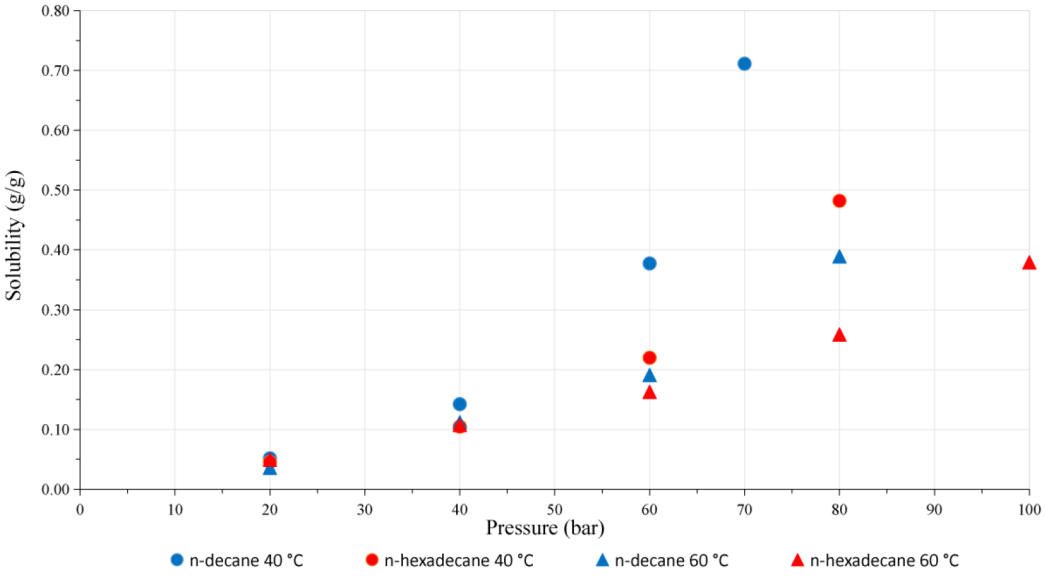

Figure 9—Calculated solubility of n-decane and n-hexadecane at 40 °C and 60 °C under different pressures.

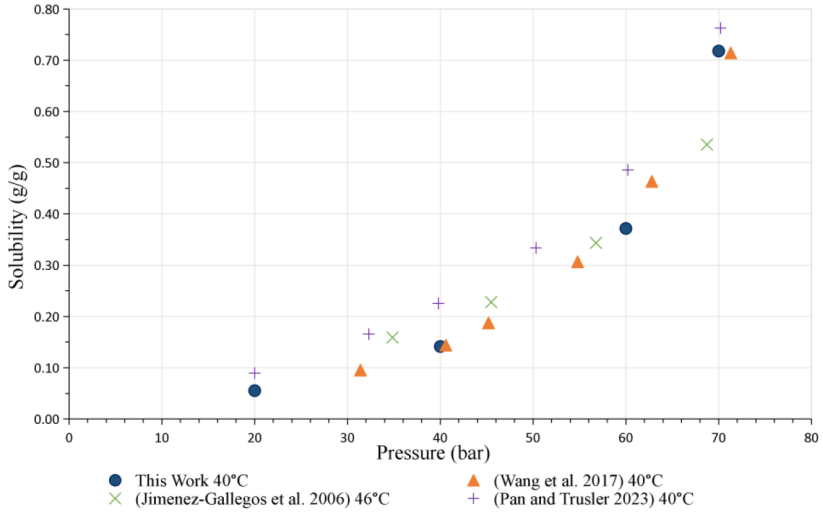

Figure 10—Solubility of CO_2 in n-decane at 40 °C and comparison with literature data.

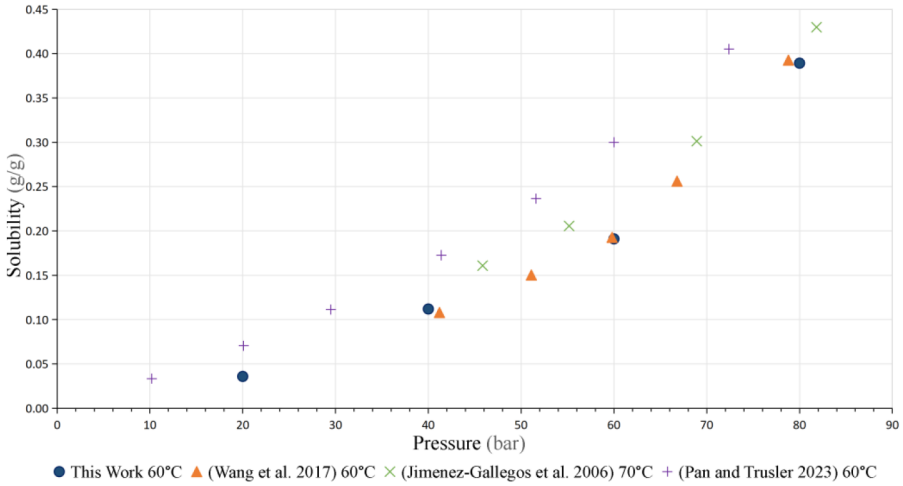

Figure 11—Solubility of CO_2 in n-decane at 60 °C and comparison with literature data.

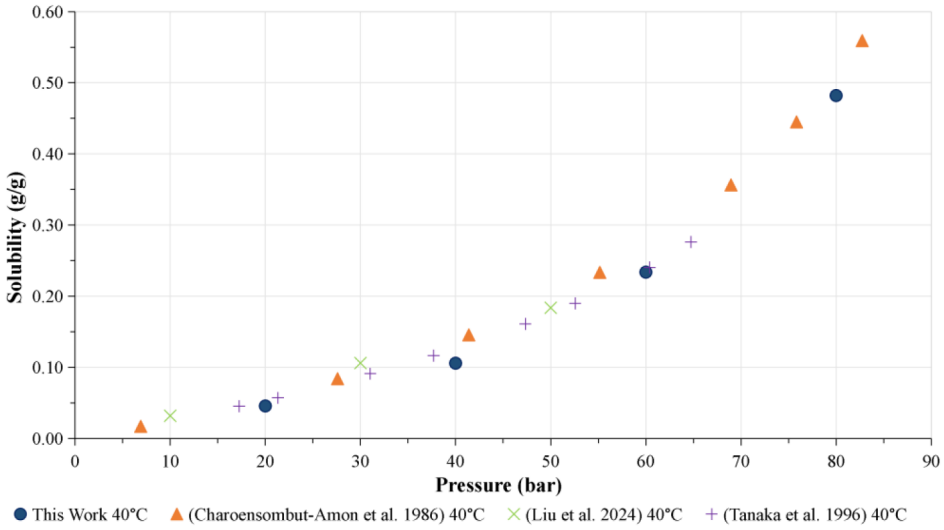

Figure 12—Solubility of CO_2 in n-hexadecane at 40 °C and comparison with literature data.

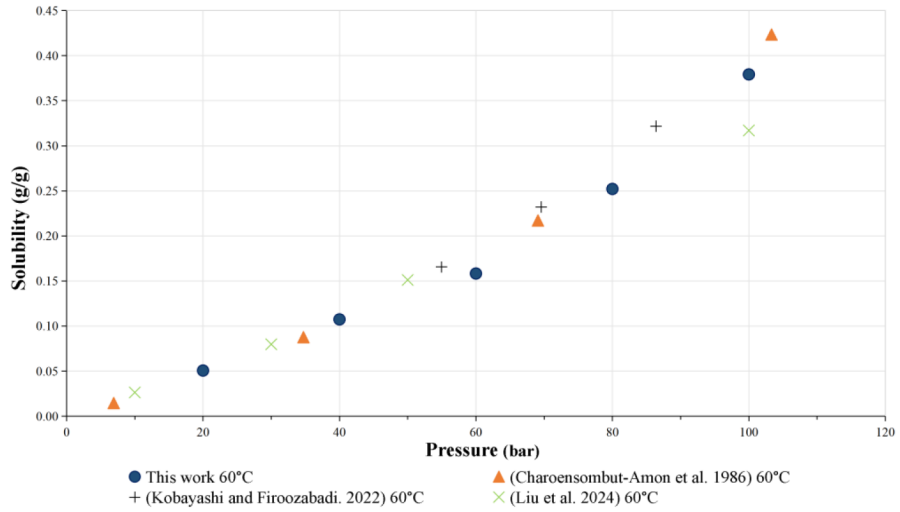

Figure 13—Solubility of CO_2 in n-hexadecane at 60 °C and comparison with literature data.

In summary, the present results show a consistent relationship between CO_2 dissolution and pressure, and exhibit good agreement with values reported previously in the literature. Increasing pressure increases both CO_2 solubility and volumetric expansion, while increasing temperature reduces CO_2 solubility and reduces droplet expansion. Shorter chain alkanes (n-decane) generally provide more free volume and looser molecular packing, which facilitates the insertion of CO_2 molecules into the hydrocarbon matrix. In contrast, longer-chain alkanes (n-hexadecane) exhibit stronger dispersive intermolecular interactions and a higher cohesive energy density, resulting in a more tightly packed structure and a higher energetic penalty for accommodating CO_2 (Han et al., 2015). This mechanistic interpretation could explain why n-decane shows higher CO_2 dissolution behavior than n-hexadecane under the same thermodynamic conditions.

Observation of continuous droplet expansion under near-miscible conditions

During the high-pressure dissolution experiments, an unexpected phenomenon was observed for both hydrocarbon systems (n-decane and n-hexadecane) at 40 °C and 60 °C. At moderate pressures, the droplet volume increased after CO_2 injection and subsequently approached a stable value, indicating that the dissolution equilibrium had been reached. However, at higher pressures, the droplet did not exhibit a clear volume plateau. An example is shown in Fig. 14 for the continuous expansion of n-decane droplet at 40

°C and 80 bar upon CO_2 dissolution. The droplet volume was observed to continue increasing, despite extending equilibration duration for times much longer than those observed for lower pressures (more than 18 hours). Under these conditions (40 °C and 80 bar), the system pressure lies in close proximity to the minimum miscibility pressure (MMP) of 87.4 bar, as reported by (Ahmadyar & Samara, 2025), where complete miscibility is attained and where the two fluids mix entirely in all proportions, forming a single homogeneous phase. At a similar pressure of 80 bar and by increasing the temperature to 60 °C, the n-decane droplet volume increased and reached a plateau which signified equilibrium as shown in Fig. 15. This is due to the direct positive correlation between temperature and MMP: higher temperatures yield higher MMP values. At 60 °C, the MMP increases to 106 bar (Ahmadyar & Samara, 2025), indicating that the system at 80 bar remains far from miscible conditions.

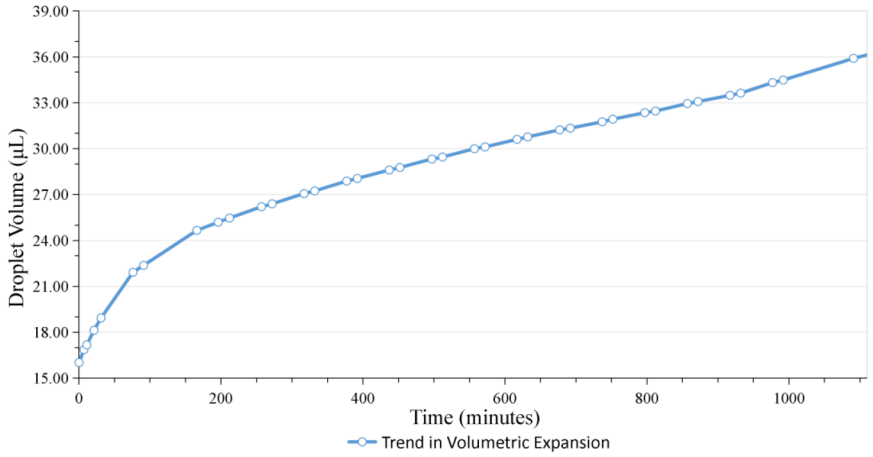

Figure 14—Continuous volumetric expansion of n-decane droplet at 40 °C and 80 bar upon CO_2 dissolution.

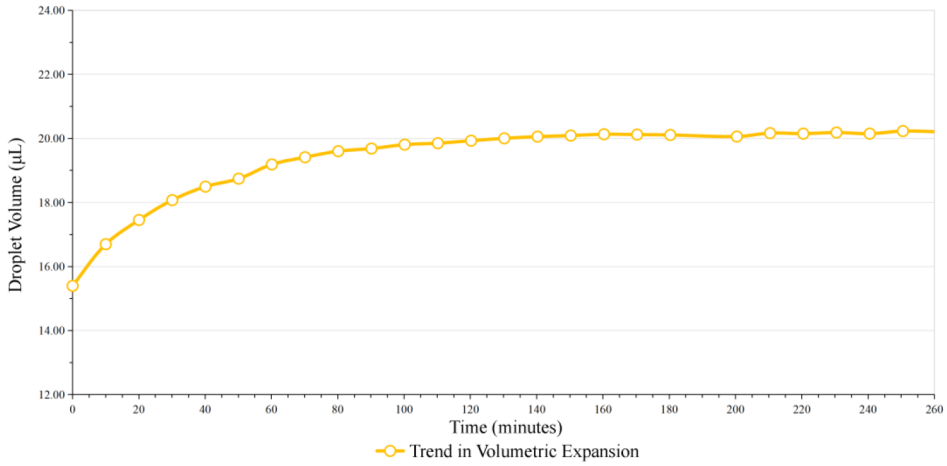

Figure 15—Volumetric expansion of n-decane droplet at 60 °C and 80 bar upon CO_2 dissolution.

Conclusions

- A systematic experimental study was conducted to investigate CO_2 dissolution-induced swelling of hydrocarbon droplets using the captive bubble method under controlled pressure and temperature conditions.
- A direct observation methodology was developed to quantify CO_2 solubility in n-decane and n-hexadecane by combining droplet volume evolution with density data, avoiding conventional compositional analysis methods.

- CO_2 solubility and droplet swelling were found to increase with pressure and decrease with temperature, consistent with thermodynamic expectations. Hydrocarbon chain length significantly influences CO_2 solubility, with n-decane exhibiting higher solubility and more pronounced swelling than n-hexadecane due to its lower cohesive energy density and looser molecular packing.
- The measured solubility values show good agreement with literature data, particularly under conditions far from the minimum miscibility pressure (MMP), confirming the reliability of the proposed methodology.
- Near-MMP conditions revealed continuous droplet expansion without reaching a plateau, indicating sustained CO_2 dissolution behavior below full miscibility.
- From an application perspective, sustained droplet swelling under near-miscible conditions may enhance oil connectivity, promote coalescence of disconnected oil ganglia, and improve displacement efficiency in CO_2-EOR processes.
- The persistence of CO_2-enriched regions within the oil phase may contribute to reduced residual oil saturation and improved sweep efficiency over time.

Acknowledgement

This work gratefully acknowledges Eurotechnica GmbH - Germany for providing access to experimental facilities and for supplying the necessary parts used in experiments performed at TU Clausthal.

References

Ahmadyar, S., & Samara, H. (2025). The effect of gas and liquid phase composition on miscibility through interfacial tension measurements of model oils in compressed CO2. *Journal of Petroleum Exploration and Production Technology*, **15**(2), 31. https://doi.org/10.1007/s13202-025-01929-5

Barclay, T. H., & Mishra, S. (2016). New correlations for CO2-Oil solubility and viscosity reduction for light oils. *Journal of Petroleum Exploration and Production Technology*, **6**(4), 815–823. https://doi.org/10.1007/s13202-016-0233-y

Charoensombutamon, T., Martin, R. J., & Kobayashi, R. (1986). Application of a generalized multiproperty apparatus to measure phase equilibrium and vapor phase densities of supercritical carbon dioxide in n-hexadecane systems up to 26 MPa. *Fluid Phase Equilibria*, **31**(1), 89–104. https://doi.org/10.1016/S0378-3812(86)87033-9

Chou, G. F., Forbert, R. R., & Prausnitz, J. M. (1990). High-pressure vapor-liquid equilibria for carbon dioxide/n-decane, carbon dioxide/tetralin, and carbon dioxide/n-decane/tetralin at 71.1 and 104.4.degree. *C. Journal of Chemical & Engineering Data*, **35**(1), 26–29. https://doi.org/10.1021/je00059a008

Fu, G.-T., Zheng, Z.-G., Zhang, Y.-Q., Dai, Y.-T., Li, D.-C., Zhan, J., Gao, C.-N., & Fan, L.-W. (2024). High-Pressure CO2 Solubility in Crude Oil and CO2 Miscibility Effects on Oil Recovery Performance in Low-Permeability Reservoirs. *Energy & Fuels*, **38**(24), 23433–23446. https://doi.org/10.1021/acs.energyfuels.4c05040

Han, H., Yuan, S., Li, S., Liu, X., & Chen, X. (2015). Dissolving capacity and volume expansion of carbon dioxide in chain n-alkanes. *Petroleum Exploration and Development*, **42**(1), 97–103. https://doi.org/10.1016/S1876-3804(15)60011-8

He, J., Xu, X., & Gui, X. (2021). New Vapor–Liquid Phase Equilibrium Data of CO2 in Several Heavy n -Alkanes at High Pressures. *Journal of Chemical & Engineering Data*, **66**(4), 1600–1610. https://doi.org/10.1021/acs.jced.0c00834

Hu, R., Crawshaw, J. P., Trusler, J. P. M., & Boek, E. S. (2017). Rheology and Phase Behavior of Carbon Dioxide and Crude Oil Mixtures. *Energy & Fuels*, **31**(6), 5776–5784. https://doi.org/10.1021/acs.energyfuels.6b01858

Jiménez-Gallegos, R., Galicia-Luna, L. A., & Elizalde-Solis, O. (2006). Experimental Vapor-Liquid Equilibria for the Carbon Dioxide + Octane and Carbon Dioxide + Decane Systems. *Journal of Chemical & Engineering Data*, **51**(5), 1624–1628. https://doi.org/10.1021/je060111z

Kobayashi, K., & Firoozabadi, A. (2022). Effect of Branching on Mutual Solubility of Alkane–CO2 Systems by Molecular Simulations. *The Journal of Physical Chemistry B*, **126**(41), 8300–8308. https://doi.org/10.1021/acs.jpcb.2c05774

Linstrom, P., & Mallard, W. G. (1997). NIST Chemistry WebBook, NIST Standard Reference Database 69 [Dataset]. *National Institute of Standards and Technology*. https://doi.org/10.18434/T4D303

Liu, X., Huang, Y., Babaei, S., Hazra, B., & Ostadhassan, M. (2024). Experimental and molecular simulation of carbon dioxide solubility in hexadecane at varying pressures and temperatures. *Chemical Engineering Journal*, **502**, 157721. https://doi.org/10.1016/j.cej.2024.157721

Mahdaviara, M., Nait Amar, M., Hemmati-Sarapardeh, A., Dai, Z., Zhang, C., Xiao, T., & Zhang, X. (2021). Toward smart schemes for modeling CO2 solubility in crude oil: Application to carbon dioxide enhanced oil recovery. *Fuel*, **285**, 119147. https://doi.org/10.1016/j.fuel.2020.119147

Mejía, A., Cartes, M., Segura, H., & Müller, E. A. (2014). Use of Equations of State and Coarse Grained Simulations to Complement Experiments: Describing the Interfacial Properties of Carbon Dioxide + Decane and Carbon Dioxide + Eicosane Mixtures. *Journal of Chemical & Engineering Data*, **59**(10), 2928–2941. https://doi.org/10.1021/je5000764

Mohammed, M., Ciotta, F., & Trusler, J. P. M. (2017). Viscosities and Densities of Binary Mixtures of Hexadecane with Dissolved Methane or Carbon Dioxide at Temperatures from (298 to 473) K and at Pressures up to 120 MPa. *Journal of Chemical & Engineering Data*, **62**(1), 422–439. https://doi.org/10.1021/acs.jced.6b00750

Nourozieh, H., Bayestehparvin, B., Kariznovi, M., & Abedi, J. (2013). Equilibrium Properties of (Carbon Dioxide + n -Decane + n -Octadecane) Systems: Experiments and Thermodynamic Modeling. *Journal of Chemical & Engineering Data*, **58**(5), 1236–1243. https://doi.org/10.1021/je4000394

Outcalt, S., Laesecke, A., & Fortin, T. J. (2010). Density and speed of sound measurements of hexadecane. *The Journal of Chemical Thermodynamics*, **42**(6), 700–706. https://doi.org/10.1016/j.jct.2010.01.003

Pan, Z., & Trusler, J. P. M. (2023). Experimental and modelling study of the interfacial tension of (n-decane + carbon dioxide + water) in the three phase region. *Fluid Phase Equilibria*, **568**, 113760. https://doi.org/10.1016/j.fluid.2023.113760

Sebastian, H. M., Simnick, J. J., Lin, H.-M., & Chao, K.-C. (1980). Vapor-liquid equilibrium in binary mixtures of carbon dioxide + n-decane and carbon dioxide + n-hexadecane. *Journal of Chemical & Engineering Data*, **25**(2), 138–140. https://doi.org/10.1021/je60085a012

Shi, Q., Jing, L., & Qiao, W. (2015). Solubility of n-alkanes in supercritical CO2 at diverse temperature and pressure. *Journal of CO2 Utilization,* **9**, 29–38. https://doi.org/10.1016/j.jcou.2014.12.002

Simoncelli, A. P. P., Goméz, W., Charin, R. M., Fleming, F. P., Ndiaye, P. M., & Tavares, F. W. (2020). Phase behavior of systems with high CO2 content: Experiments and thermodynamic modeling. *Fluid Phase Equilibria*, **515**, 112574. https://doi.org/10.1016/j.fluid.2020.112574

Siqueira Campos, C. E. P., Villardi, H. G. D., Pessoa, F. L. P., & Uller, A. M. C. (2009). Solubility of Carbon Dioxide in Water and Hexadecane: Experimental Measurement and Thermodynamic Modeling. *Journal of Chemical & Engineering Data*, **54**(10), 2881–2886. https://doi.org/10.1021/je800966f

Tanaka, H., Yamaki, Y., & Kato, M. (1993). Solubility of carbon dioxide in pentadecane, hexadecane, and pentadecane + hexadecane. *Journal of Chemical & Engineering Data*, **38**(3), 386–388. https://doi.org/10.1021/je00011a013

Wang, J., Zhang, Z., Wang, Q., Lou, T., Pan, Z., & Hu, M. (2023). Integrated a Fused Silica Capillary Cell and In Situ Raman Spectroscopy for Determining the Solubility of CO2 in n-Decane and n-Decane + n-Hexane System. *Processes*, **11**(4), 1137. https://doi.org/10.3390/pr11041137

Wang, J., Zhou, S., Bei, K., Zhang, D., Chou, I.-M., Chen, Z., Lin, C., & Pan, Z. (2017). Using a Fused Silica Capillary Cell and In Situ Raman Spectroscopy To Develop a Setup for Measurement of the Volume Expansion of Carbon Dioxide + n -Hexane. *Energy & Fuels*, **31**(6), 6314–6319. https://doi.org/10.1021/acs.energyfuels.7b00549